Observing and Modeling Multifrequency Scattering of Maize During the Whole Growth Cycle

Andrea Della Vecchia, Paolo Ferrazzoli, *Senior Member, IEEE*, Leila Guerriero, Luca Ninivaggi, Tazio Strozzi, *Senior Member, IEEE*, and Urs Wegmüller, *Senior Member, IEEE*

***Abstract*—The objective of this paper is to carry out a systematic investigation about the sensitivity of radar to maize crop growth and soil moisture by considering a wide range of frequencies and angles and all linear polarizations. We show the results of a correlation study carried out on the data collected on a maize field at Suberg, in the Swiss region named Central Plain, by the multifrequency RAdio ScAtteroMeter (RASAM). This agricultural field was monitored over a long period of time at a wide range of frequencies and observation angles so that the correlation between the backscattering and crop height and the biomass and soil moisture was studied under several plant and observation conditions. Moreover, we describe some recent refinements applied to the vegetation scattering model developed at Tor Vergata University, Rome, Italy, and we evaluate the accuracy of extended comparisons between model outputs and RASAM signatures. The Tor Vergata model is finally applied to give a theoretical basis to the experimental correlation findings.**

***Index Terms*—Biomass, crops, modeling, radar, soil moisture.**

I. Introduction

In RECENT years, important advances have been achieved toward understanding the interaction processes between microwaves and crops; at the same time, crop monitoring techniques based on radar observations are progressing. An important opportunity has been offered by the expanded availability of spaceborne SAR data. By analyzing multitemporal signatures collected during overpasses of ERS-1, ERS-2, JERS-1, Radarsat-1, and Envisat over large agricultural areas, several issues related to microwave scattering of various crops have been investigated [1]–[7]. In addition, ground-based and airborne measurements have contributed significantly [8]–[10]. Moreover, indoor measurements have improved our understanding of scattering contributions due to single components, that is soil, lower canopy and upper canopy [11]–[13]. Important advances have also been achieved in modeling. Some efforts have been focused on coherent combinations of scattering contributions [14], analyzing the situations for which these effects may be important, particularly at L-band. In addition, the description of single scatterers has been improved [15], [16], and models have been tested using new campaigns with detailed ground truth, including geometrical variables [6]. All these efforts are aimed at improving monitoring techniques. From this point of view, the advantages offered by the use of backscattering polarization indexes have been investigated [17]. It is also recognized that soil and vegetation variables must be estimated simultaneously. This is desirable for several applications; however, it is also necessary to improve the accuracy of the estimates because both soil and vegetation scattering contribute to the overall crop backscattering. It is difficult to solve these problems with radar operating with a single configuration (in terms of frequency, polarization, and angle), whereas it is recognized that a dual-polarization system may have a better chance than a single-polarization one.

However, some limits are still present in the state of the art, and further efforts are needed. First of all, most presently available spaceborne radar signatures are at C-band. As a consequence of this, theoretical and application efforts in data analysis, modeling, and monitoring techniques have been focused on this band. However, the exploitation of valid algorithms is limited when only a single frequency is used, particularly if various crops are considered. On the other hand, present and future spaceborne systems allow us to work with a significantly expanded microwave spectrum (from L- to X-band). This has to be considered in further experimental and modeling studies. Moreover, investigations about angle and polarization effects, using spaceborne data, suffer limitations, considering that SAR instruments mounted on ERS-1, ERS-2, and Radarsat-1 operate at a single polarization and at, essentially, a single-look angle. Important improvements have been achieved with Envisat ASAR; however, for a specific angle and polarization pair, the revisit time is generally poor. This limits the capability to derive multitemporal trends in spite of efforts made by the investigators (see, e.g., [7]). Therefore, backscattering data collected in old scatterometer campaigns, although limited to single fields, are still useful for investigating multitemporal trends in detail.

For the dimensioning of future systems, it is important to find convenient radar configurations. Some concepts, such as the prevalence of soil scattering at low frequencies and low angles and the prevalence of canopy scattering at high frequency and high angles, are well established and valid for all crops. Some discussions about different properties related to crop geometry have been developed [18]; however, systematic and widely agreed conclusions have not yet been achieved.

Manuscript received December 12, 2007; revised April 18, 2008. Current version published October 30, 2008.

A. Della Vecchia, P. Ferrazzoli, and L. Guerriero are with the Department of Computer Science, Systems and Industrial Engineering, Faculty of Engineering, Tor Vergata University, 00133 Rome, Italy (e-mail: dellavecchia@disp.uniroma2.it; ferrazzoli@disp.uniroma2.it; guerriero@disp.uniroma2.it).

L. Ninivaggi was with the Department of Computer Science, Systems and Industrial Engineering, Faculty of Engineering, Tor Vergata University, 00133 Rome, Italy. He is now with Accenture, 00142 Rome, Italy (e-mail: lucaninivaggi@libero.it).

T. Strozzi and U. Wegmüller are with GAMMA Remote Sensing, 3073 Gümligen, Switzerland (e-mail: strozzi@gamma-rs.ch; wegmuller@gamma-rs.ch).

Digital Object Identifier 10.1109/TGRS.2008.2001885

TABLE I
TOTAL NUMBER OF MEASUREMENTS AT EACH FREQUENCY AND AT EACH DAY OF OBSERVATION

Day of Year	2.5 GHz	3.1 GHz	4.6 GHz	7.2 GHz	10.2 GHz
123	15	15	14	15	15
127	15	15	12	15	15
132	15	15	12	15	15
139	15	15	15	15	15
145	15	15	11	15	15
151	15	15		15	15
155	15	15		15	15
159	15	15	15	15	15
162	15	15	12	15	15
166	15	15	15	15	15
167	15	15	15	15	15
175	15	4		15	15
180	15	15		13	15
186	15		15	15	15
193	15	15	15	15	15
200	15	15	12	15	15
253	10	10	15	15	15
256	4	4	15	15	15
263	5	5	15	15	15
279	15	15	15	15	15
285	10	10	10	10	10
291	15	15	15	15	15
298	10	10	10	10	10

In this paper, previous studies about maize scattering at C-band [6] are significantly expanded. Comparisons between model simulations and experimental data collected by RAdio ScAtteroMeter (RASAM) [19], [20] are presented, covering a complete growth cycle, a frequency range between 2.5 and 10.2 GHz, an angle range between 20° and 50°, and at VV, HH, and HV polarizations. Results of the study lead to considerations about convenient configurations for crop monitoring. Section II introduces the experimental data set and the statistical study carried out on maize. In Section III, the main concepts of the maize scattering model are summarized; an already developed model [21], with some refinements and/or semiempirical corrections, is used. These modifications aim at improving backscattering simulations using variables measured on the field. Section IV shows a critical comparison between experimental and simulated signatures, and the results are used to develop considerations about convenient radar parameters.

II. EXPERIMENTAL DATA SET AND APPLICATION ASPECTS

A statistical study has been carried out on radar signatures collected in Switzerland by the RASAM in 1988. Details about the instrument and the campaigns are given in [19]. Since measurements were ground based, observations were confined to a single field; however, in spite of this limitation, the data set is very useful because it covers a wide range of frequencies, angles, and the three linear polarizations. In this work, we consider the backscattering coefficient per unit area σ^0 (in square meter per square meter) measured over a maize field at 2.5, 3.1, 4.6, 7.2, and 10.2 GHz. For each frequency, we considered the five observation angles of 20°, 30°, 40°, 50°, and 60° and the VV, HH, and HV polarizations. Measurements of the backscattering coefficient were collected during the whole crop cycle at the days of year (DoY) reported in Table I, where the total number of measurements acquired each day for each frequency is also reported. This number is equal to a maximum of 15 when measurements at all the five angles and the three polarizations were available. Depending on the observation parameters, i.e., frequency, angle, and polarization, data are available for a minimum of 11 days and a maximum of 21 days.

TABLE II
PHENOLOGICAL STAGES OF THE MAIZE FIELD

Day of Year	Date	Stage
126	May 5	Sowing
135	May 14	Germination
198	July 16	Bloom, growth of cobs
205	July 23	End of growth
275	October 1	Yellowing of leaves
298	October 24	Harvest

The phenological evolution of the maize field at Central Plain is described in Table II; however, ground measurements of some important variables of the crop fields were also carried out simultaneously to the scatterometer measurements, namely, volumetric soil moisture, crop biomass, crop height (which are shown in Fig. 1 versus the day of measurements), and vegetation moisture.

The sensitivity of RASAM signatures to crop height, biomass, and soil-moisture content (SMC) has been analyzed by means of the correlation coefficient. The latter has been estimated, assuming a quadratic regression between the independent variable and the three linear polarizations, or a combination of them, i.e., their ratios, at the five frequencies and five angles mentioned previously. When calculating the correlation with crop parameters, the data set collected over the whole growth cycle (from DoY 123 to 298) has been included in the estimation; when considering soil moisture, only the samples collected during the growth phase have been taken into account, i.e., until the highest value of height (or biomass) has been reached (from DoY 123 to 253). The results are reported by means of gray-level diagrams (Figs. 2–6) with the frequency and incidence angle on the vertical and horizontal axes, respectively. Figs. 2 and 3 show correlation coefficients with respect to soil moisture of backscattering coefficients and polarization ratios, respectively. Figs. 4 and 5 show the coefficients computed with respect to crop height. For the case of polarization ratios, the correlation coefficients, with respect to biomass, are also shown in Fig. 6. The light shades of gray represent high correlation coefficients, whereas dark shades represent low correlation coefficients. The black squares with a white cross replace unreliable values of the correlation coefficient, which are obtained when only ten, or less than ten, measurements are available.

The diagrams show that the highest correlations with soil moisture are presented by the copolar backscattering coefficients at low frequencies and low angles, in agreement with several previous studies (see, for example, [22, p. 1872]). In particular, correlations higher than 0.75 are seen in the σ^0_{VV} (Fig. 2), whereas the correlations between the polarization ratios and soil moisture are rather weak.

If single polarizations are taken into account, low correlation coefficients, with respect to maize vegetation parameters, are

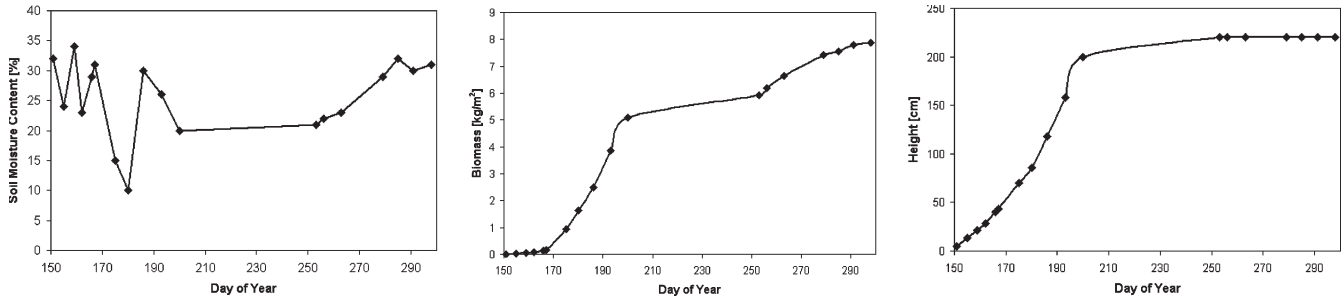

Fig. 1. Variables measured on the Central Plain maize field. From left to right: SMC, biomass, and plant height.

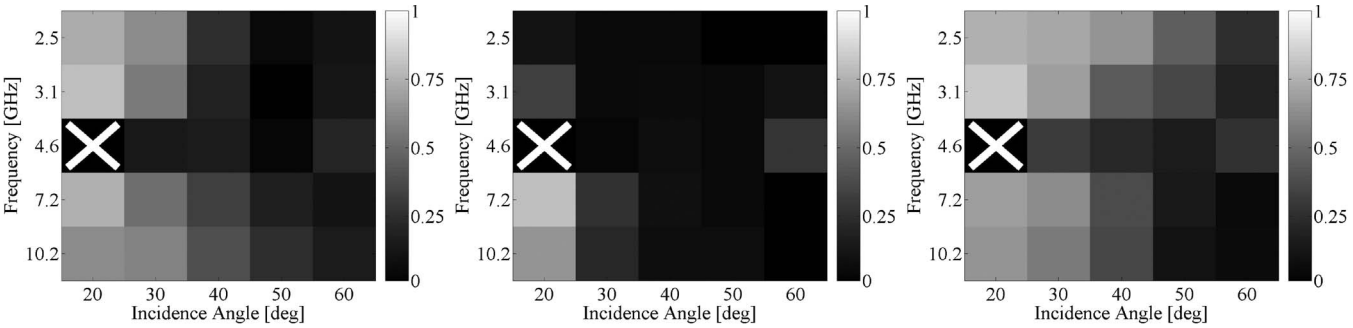

Fig. 2. Correlation of backscattering coefficient with SMC in the maize field as a function of frequency and observation angle. From left to right: HH, HV, and VV polarizations.

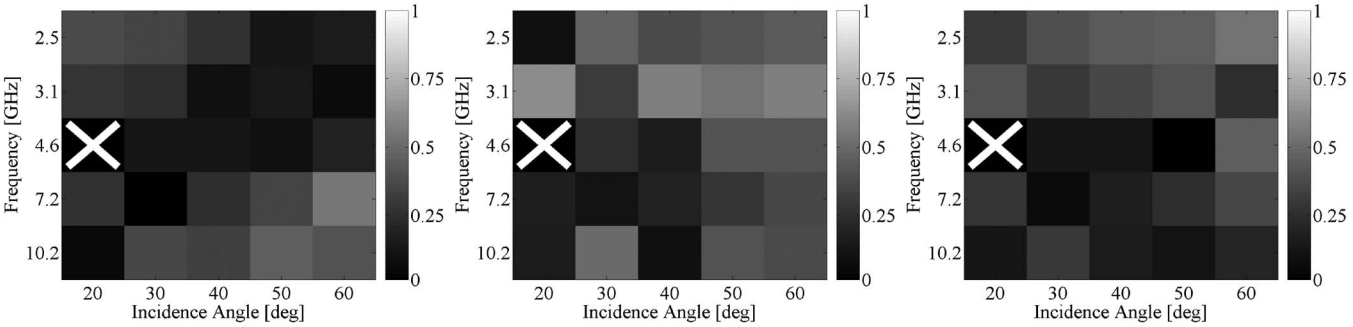

Fig. 3. Correlation of backscattering coefficient ratios with SMC in the maize field as a function of frequency and observation angle. From left to right: HH/HV, VV/HH, and VV/HV.

observed (Fig. 4), except for some isolated peaks at angles $> 50^\circ$. These good correlations are related to the preponderance of vegetation contribution; however, angles higher than 50° are seldom used in operational systems. Good correlations (larger than 0.7) with maize biomass and height are achieved by the copolar $\sigma^0_{\rm VV}/\sigma^0_{\rm HH}$ and the cross-polar $\sigma^0_{\rm VV}/\sigma^0_{\rm HV}$ ratios at C-band and observation angles $> 30^\circ$, in agreement with model simulations performed in [17]. We stress that comparable correlation values are obtained at low angles $(20^\circ$–$30^\circ)$ and low frequencies (typically S-band) by $\sigma^0_{\rm VV}/\sigma^0_{\rm HV}$. This turns out to be an interesting result because of the previously mentioned sensitivity of the VV polarization to the SMC at this radar configuration. By looking at Fig. 6, it can be noticed that the results of correlations with respect to the biomass are similar to the case of the correlation with respect to the height.

In Fig. 7, the correlation between the polarization ratios and the wheat biomass is represented; the previous considerations concerning maize parameters can also be drawn in the case of wheat. It can be pointed out that the C-band copolar ratio at 40°, suggested in [11] as a suitable parameter for wheat biomass retrieval, shows a significant correlation value. However, the cross-polar ratio at low angles and low frequencies shows a good potential also in the case of wheat.

Examples of useful experimental trends are shown in Fig. 8, where the $\sigma^0_{\rm VV}/\sigma^0_{\rm HV}$ ratio, measured at 2.5 GHz and 20° incidence angle over the maize field, is studied versus both the crop height and biomass, with the latter being the most significant parameter from the application point of view. Superimposed to the experimental data, the regression curves obtained by the quadratic fitting are reported.

In general, the cross-polarization ratios are particularly high for bare soils due to the high values of the copolar backscattering coefficient and decrease appreciably during crop growth due both to the decreasing trend of the copolar smashσ^0 and the increasing trend of the cross-polar σ^0. At low frequencies and low angles, the dynamic range of the polarization ratio is on the order of 8–10 dB, whereas variations of soil moisture and vegetation structure produce more limited effects. From Fig. 8, it

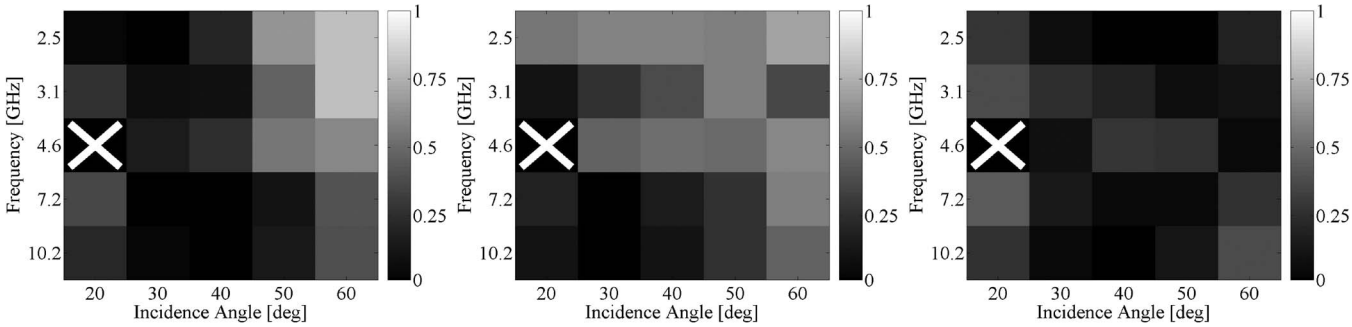

Fig. 4. Correlation of backscattering coefficient with plant height as a function of frequency and observation angle. From left to right: HH, HV, and VV polarizations.

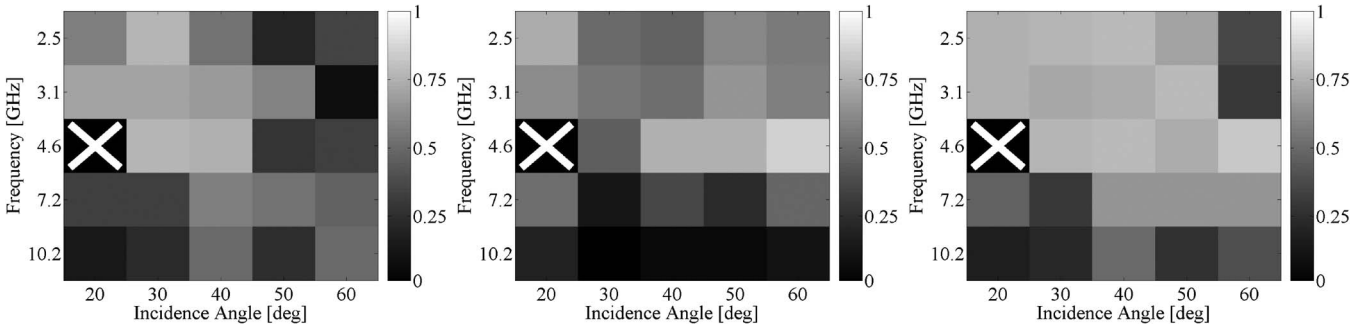

Fig. 5. Correlation of backscattering coefficient ratios with plant height as a function of frequency and observation angle. From left to right: HH/HV, VV/HH, and VV/HV.

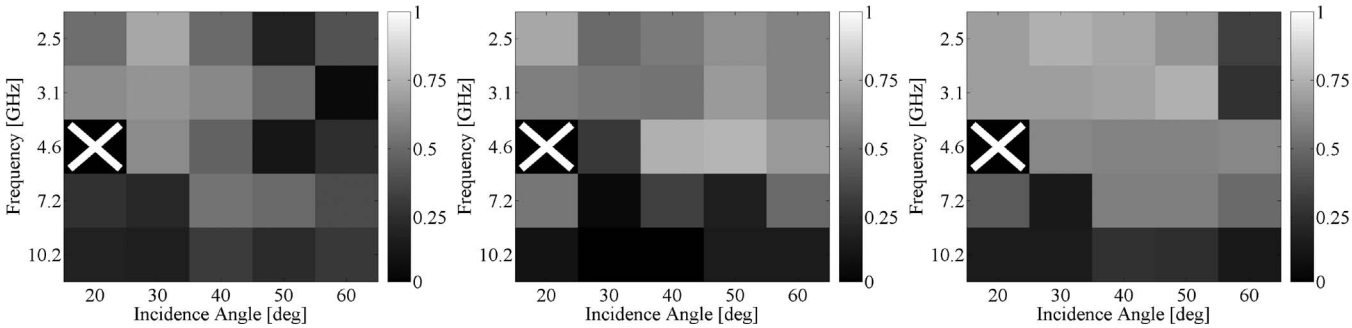

Fig. 6. Correlation of backscattering coefficient ratios with maize biomass as a function of frequency and observation angle. From left to right: HH/HV, VV/HH, and VV/HV.

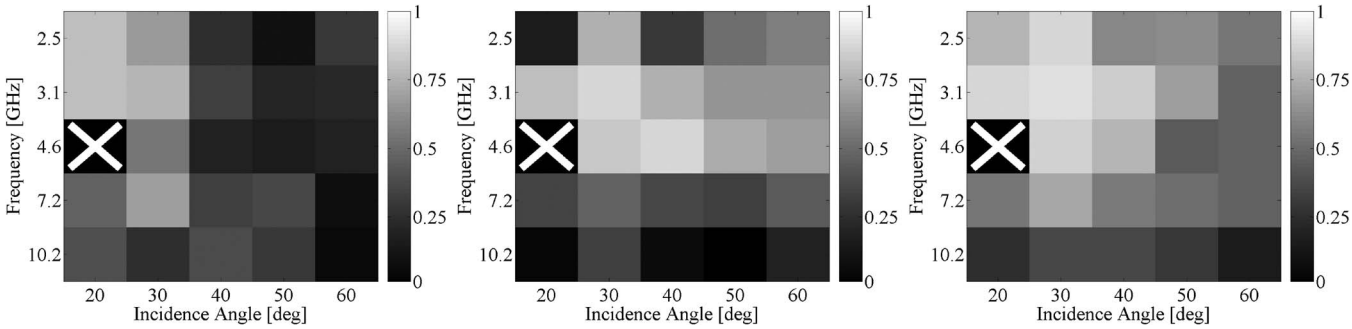

Fig. 7. Correlation of backscattering coefficient ratios with wheat biomass as a function of frequency and observation angle. From left to right: HH/HV, VV/HH, and VV/HV.

can be observed that for very low height values, a first decrease of $\sigma^0_{\mathrm{VV}}/\sigma^0_{\mathrm{HV}}$ is observed, whereas no significant biomass variation is present; this is due to the development of maize leaves in the early phase of growth, which produces a change of backscattering without a significant biomass increase.

III. Modeling Issues

A. General Aspects

In this paper, a discrete scattering model is used. The advantages of the discrete modeling approach are generally

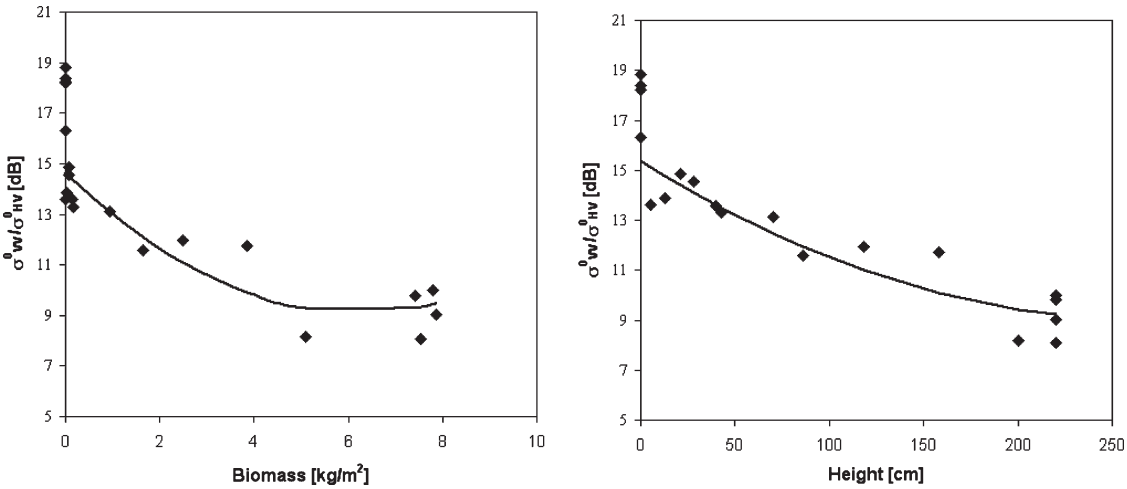

Fig. 8. Experimental trend of $\sigma^0_{\rm VV}/\sigma^0_{\rm HV}$ as a function of (left) biomass and (right) crop height at 2.5 GHz and 20° incidence angle. The continuous line represents the quadratic regression.

recognized; discrete models represent the fundamental properties of single-vegetation elements, and allow us to combine scattering contributions using well-established theories.

The basic algorithm is described in [21], and some advanced implementation aspects are introduced in [6]. Here, some main concepts are summarized. Leaves are described by dielectric discs, and stems and ribs by dielectric cylinders. For each scatterer, dimensions, orientation, and permittivity are required as input. For discs, the scattering and extinction cross sections are computed using the Rayleigh–Gans theory [23] up to 5 GHz and the physical optics theory [24] at higher frequencies. The theory based on the "infinite length" approximation [25] is used for ribs and stems. The scatterer location within the canopy is selected in order to reproduce, as far as possible, the real crop geometry. Discs and randomly oriented thin cylinders, representing leaves and ribs, respectively, are placed in an upper layer; a lower layer with vertical cylinders is used for the stems over the soil, which is represented by a rough dielectric surface. The Integral Equation Model [26] is used to compute the bistatic scattering coefficient of soil. Single scatterers' contributions are combined by using a matrix algorithm, which is also used to combine vegetation scattering with soil scattering. Finally, the canopy backscattering coefficient at pq polarization is obtained.

The simulated backscattering coefficient may be decomposed into three main components, as indicated in

$$\sigma^0_{pq} = \left[\sigma^0_{pq}\right]_{\rm V} + \left[\sigma^0_{pq}\right]_{\rm VS} + T_p \left[\sigma^0_{pq}\right]_{\rm S} T_q \qquad (1)$$

where

σ^0_{pq}	whole canopy backscattering coefficient;
$[\sigma^0_{pq}]_{\rm V}$	vegetation direct backscattering component;
$[\sigma^0_{pq}]_{\rm VS}$	soil–vegetation interaction backscattering component, including double-bounce effects;
$[\sigma^0_{pq}]_{\rm S}$	backscattering component due to bare soil;
T_p and T_q	canopy transmissivities at the p and q polarizations, respectively.

In this paper, a specific semiempirical modification has been applied to correct surface model inaccuracies in simulating the cross-polarized backscattering of soils. In fact, although several advances have been achieved in representing the statistics and the electromagnetic properties of soil surfaces, these efforts improved the description of copolarized backscattering only [27], [28]; however, the soil backscattering coefficient measured at the HV polarization is still clearly underestimated by surface models (see, e.g., [29]). Research on this subject is still in progress, and for the time being, we have adopted the semiempirical method indicated in the following.

The scatterometer acquisition samples have been subdivided into two ensembles. The first ensemble includes the first N_1 samples collected before crop emergence (which includes DoY from 123 to 145), whereas the second one includes the N_2 samples collected in the presence of vegetation (from DoY 151 to 298).

TABLE III
MEASURED COVER FRACTION OVER THE MAIZE FIELD

Day of Year	Coverage fraction
151	0.05
155	0.05
159	0.12
162	0.2
166	0.23
167	0.25
175	0.3
180	0.35
186	0.5
193	0.65
200	0.8
253	0.8
256	0.8
263	0.8
279	0.8
285	0.8
291	0.8
298	0.8

TABLE IV
MEASURED SMC OVER BARE SOIL BEFORE EMERGENCE OF THE MAIZE FIELD

Day of Year	SMC [%]
123	22
127	18
132	32
139	33
145	22

TABLE V
CORRECTION RATIOS $[\sigma^0_{\rm HV}/\sigma^0_{\rm VV}]_1$ AT THE FREQUENCIES AND ANGLES CONSIDERED IN THE MODEL COMPARISON AGAINST EXPERIMENTAL DATA

Frequency [GHz]	*20°*	*30°*	*40°*	*50°*
2.5	-16.47	-11.57	-10.51	-9.02
3.1	-14.55	-12.04	-11.91	-11.94
4.6	-11.83	-11.37	-11.85	-10.5
7.2	-10.87	-9.52	-9.22	-8.6
10.2	-10.13	-9.52	-10.01	-8.93

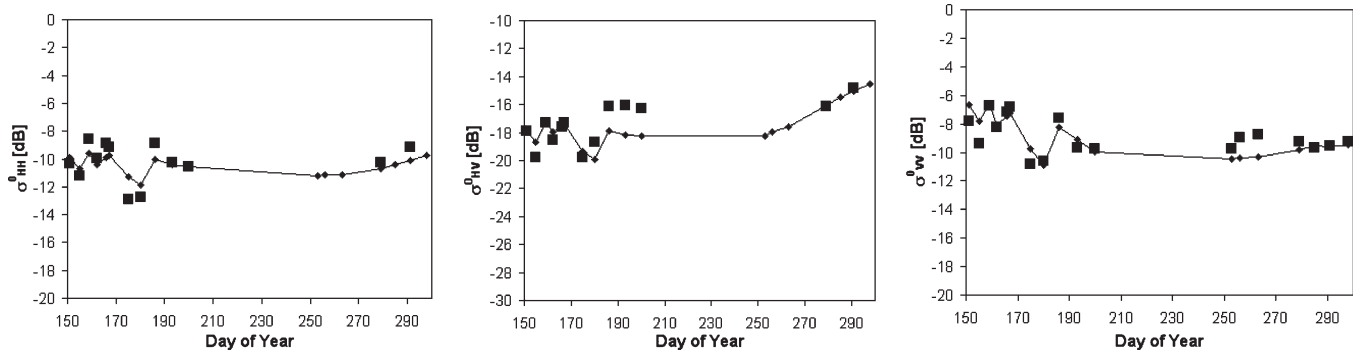

Fig. 9. Comparison between (continuous line) simulated and (squares) measured data at 2.5 GHz and $\vartheta_i = 30°$. From left to right: HH, HV, and VV polarizations.

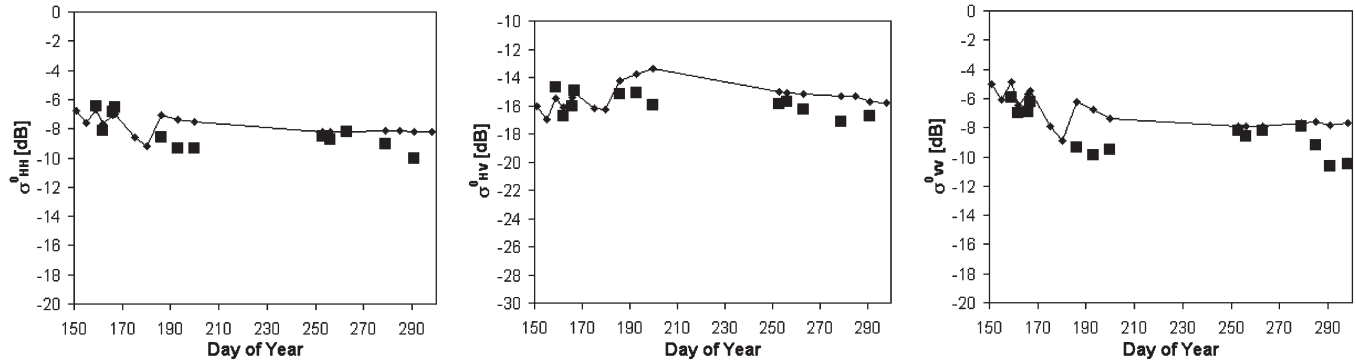

Fig. 10. Comparison between (continuous line) simulated and (squares) measured data at 4.6 GHz and $\vartheta_i = 30°$. From left to right: HH, HV, and VV polarizations.

For each frequency and angle, we have computed the average ratio between HV and VV backscattering coefficients before crop emergence

$$\left[\frac{\sigma^0_{\rm HV}}{\sigma^0_{\rm VV}}\right]_1 = \frac{1}{N_1}\sum_{i=1}^{N_1}\frac{\sigma^0_{{\rm HV}i}}{\sigma^0_{{\rm VV}i}} \tag{2}$$

where the index i indicates a collected scatterometer sample of the first ensemble (with N_1 samples).

Afterwards, we have computed the HV backscattering coefficient at different stages of the crop cycle ($j = 1, 2, \ldots, N_2$), which will be considered in the following analysis. For each scatterometer sample j of the second ensemble (with N_2 samples), the application of (1) has been modified as:

$$\sigma^0_{\rm HV}(j) = \left[\sigma^0_{\rm HV}\right]_{\rm V}(j) + \left[\sigma^0_{\rm HV}\right]_{\rm VS}(j) + T_{\rm H}(j)\left[\sigma^0_{\rm VV}\right]_{\rm S}(j)\left[\frac{\sigma^0_{\rm HV}}{\sigma^0_{\rm VV}}\right]_1 T_{\rm V}(j) \tag{3}$$

where the HV-polarized backscattering coefficient of bare soil is calculated on the basis of the theoretical $[\sigma^0_{\rm VV}]_{\rm S}$ corrected by the average ratio of (2).

No modifications have been applied to the copolar σ^0's of bare soil. It is stressed that although this is a semiempirical operation, it is not a mere fitting. In fact, $[\sigma^0_{\rm HV}/\sigma^0_{\rm VV}]_1$ values are computed *a priori* with respect to vegetation growth, using an independent data set. Therefore, the samples adopted to compute them are kept apart from the samples adopted to test the crop scattering models.

B. Model for Maize

The model requires, as input, the geometric and dielectric variables of soil and vegetation. We have used the measured ones and, if not available, we have estimated them by using a growth routine fitted over measurements of previous campaigns. In particular, the geometrical variables used for stems and leaves are the same as in [6, Table 1], where C-band tests were performed. Here, long leaves have been subdivided into several discs, with the diameter equal to the leaf width, which

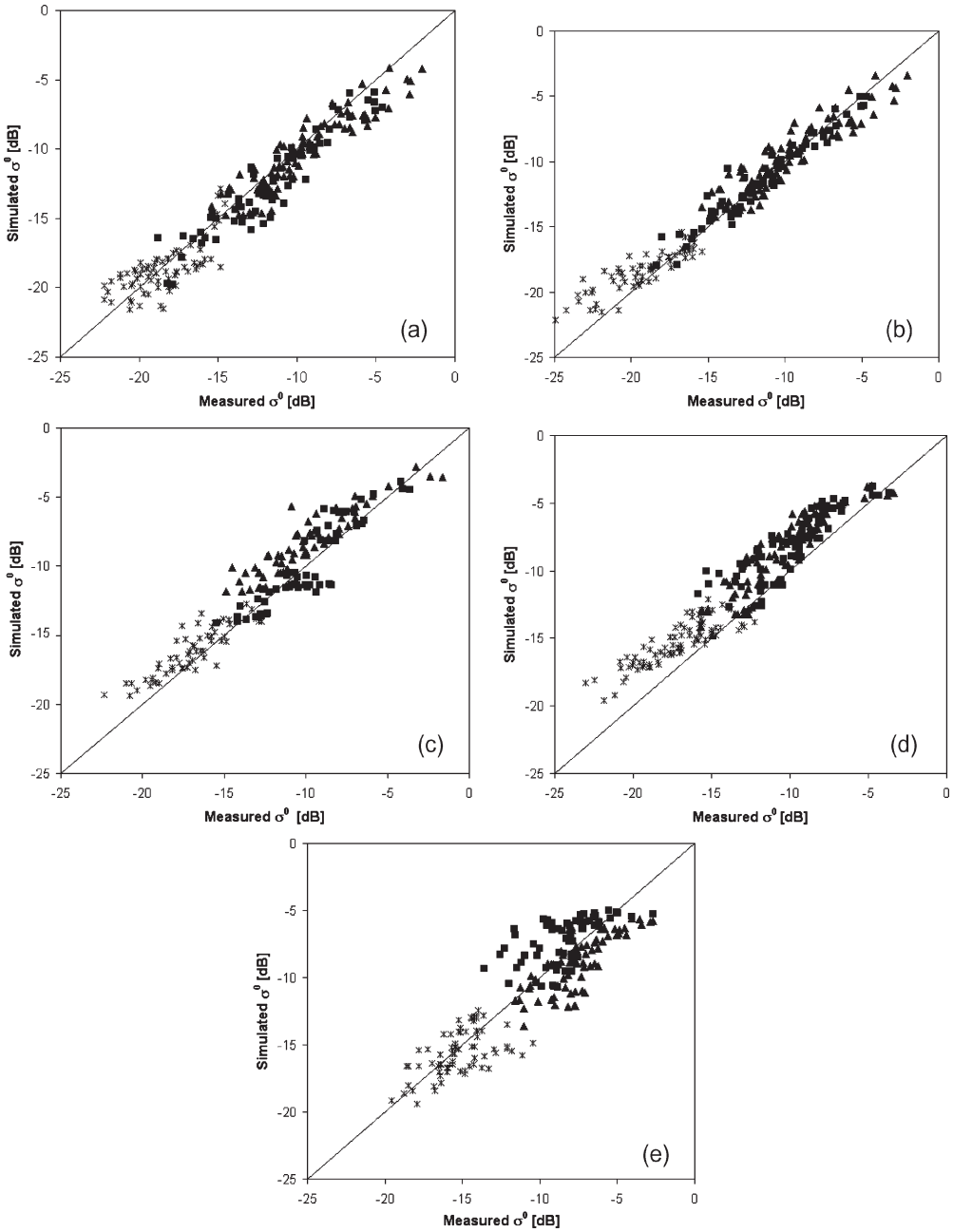

Fig. 11. Comparison between simulated and measured backscattering coefficients at (a) 2.5, (b) 3.1, (c) 4.6, (d) 7.2, and (e) 10.2 GHz. Angles are at 20°, 30°, 40°, and 50°. (Triangles) σ^0_{VV}. (Squares) σ^0_{HH}. (Stars) σ^0_{HV}.

corresponds to the simpler assumption within the alternatives proposed in [6]. Furthermore, the ribs present in the maize leaves have been modeled by means of cylinders having a diameter equal to 0.3 cm and length equal to the leaf half-length. Two cylinders per leaf have been considered.

A further modification to the model has been applied to consider that in the early stage, vegetation elements are not uniformly distributed over the soil but tend to thicken along the rows. This is confirmed by the coverage fraction measurements C, which indicate low values at the early stage (see Table III). We assumed that a fraction C of the observed area is covered by vegetation with a higher density than the average one that was measured, and that the remaining fraction $(1-C)$ has a null scatterer density. In order to consider this effect, we have applied the correction indicated in the following.

For each observation sample j, the average number of stems and leaves per unit area measured on the site ($n_{\mathrm{s}j}$ and $n_{\mathrm{l}j}$, respectively) have been modified into $n_{C_{\mathrm{s}}j}$ and $n_{C_{\mathrm{l}}j}$ based on $n_{C_{\mathrm{s}}j} = n_{\mathrm{s}j}/C_j$ and $n_{C_{\mathrm{l}}j} = n_{\mathrm{l}j}/C_j$, where C_j is the coverage fraction, which varies with the DoY as reported in Table III. This way, the concentration of scatterers in a limited fraction of the observed area has been taken into account.

By using the $n_{C_{\mathrm{s}}j}$ and $n_{C_{\mathrm{l}}j}$ densities, the backscattering coefficient $\sigma^0_{C_{pq}}(j)$ within the vegetation-covered area is computed based on (1) or (3), respectively, for co- and cross-polar simulations.

TABLE VI
RMS ERRORS BETWEEN MEASURED AND SIMULATED σ^0 VALUES AT THE FIVE FREQUENCIES CONSIDERED

Frequency [GHz]	Rms error [dB]
2.5	1.39
3.1	1.37
4.6	1.57
7.2	2.23
10.2	1.91

Given the theoretical bare-soil backscattering coefficient $[\sigma^0_{pq}]_{\rm S}(j)$, the total backscattering coefficient $\sigma^0_{Tpq}(j)$ is finally calculated as the sum of two terms

$$\sigma^0_{Tpq}(j) = \sigma^0_{Cpq}(j) \cdot C_j + \left[\sigma^0_{pq}\right]_{\rm S}(j) \cdot (1 - C_j). \quad (4)$$

The first term is the backscattering coefficient of the C_j fraction of area which is covered by vegetation, and the second one is the backscattering coefficient of the $(1 - C_j)$ fraction of bare soil.

IV. COMPARISONS WITH MULTIFREQUENCY DATA

The model, with the modifications described in the previous section, has been extensively tested using experimental data collected by RASAM, and used in Section II for the correlation study. In this section, we compare experimental radar signatures with simulations performed using the *in situ* measured cover fractions of Table III.

Bare soil samples collected on $N_1 = 5$ days before corn crop growing are used to recalibrate the theoretical soil HV backscattering coefficient, based on the semiempirical procedure described in Section III-A. The volumetric SMC measured by the five samples are reported in Table IV, and the averaged ratios $[\sigma^0_{\rm HV}/\sigma^0_{\rm VV}]_1$ are listed in Table V, as a function of the frequency and angle.

Model simulations, as a function of the day of measurements, are compared against RASAM data in Figs. 9 and 10, namely, for frequencies $f = 2.5$ and 4.6 GHz and incidence angle $\vartheta_i = 30^\circ$. In general, the model follows, fairly well, the plant growth; larger backscattering variations occur in the first days when the maize biomass is low because of soil-moisture change, whereas smaller variations are observed afterward.

Overall comparisons at 2.5, 3.1, 4.6, 7.2, and 10.2 GHz are shown in Fig. 11. These plots include all samples at 20°, 30°, 40°, 50°, and VV, HH, and HV polarizations. Total rms error values for all frequencies are given in Table VI. At 2.5 GHz, the higher discrepancies are observed for large σ^0 values, i.e., at lower angles, where the soil contribution is more important, whereas a systematic overestimation (on the order of 1–2 dB) is observed at 7.2 GHz. In general, the absolute discrepancies are limited, and the dynamic range related to crop growth and to the variations of angle and polarization is well represented. This is important, considering that in the following, we show how the model confirms that the use of a polarization pair at low angles is convenient for crop monitoring.

The previous statistical study has demonstrated that correlations larger than 0.7, with both soil moisture and maize height or biomass, are shown by radar configurations at low frequencies and low angles. Thus, we have run the model at 2.5 GHz and 20°, and the simulated values of $\sigma^0_{\rm VV}/\sigma^0_{\rm HV}$ are shown in Fig. 12 as a function of crop height, which is the driving parameter of the electromagnetic model. Bare-soil values of the ratio are assigned by the procedure illustrated in Section III-A. In the analysis shown in Fig. 12, we have investigated how the sensitivity to crop growth may be affected by soil-moisture variations. For each day of observation, the backscattering coefficient of maize has been simulated by means of the model, improved as described in Section III-B in order to take the coverage parameter into account. In order to single out the vegetation and soil scattering effects, the SMC has been kept constant in each temporal simulation; however, the time trends have been simulated under four different soil-moisture conditions.

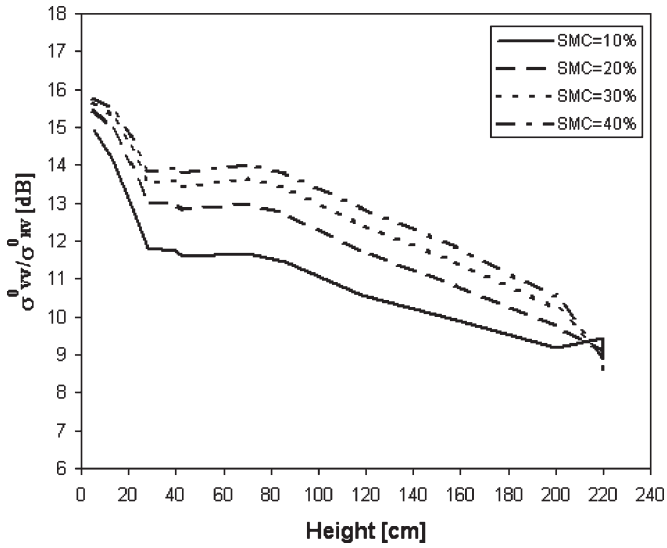

Fig. 12. Simulated trends of $\sigma^0_{\rm VV}/\sigma^0_{\rm HV}$ as a function of the maize height at 2.5 GHz and 20° incidence angle for constant values of volumetric soil moisture.

The simulated ratios in Fig. 12 reproduce the decreasing trend observed experimentally; these ratios are particularly high for bare soils due to the high values of $\sigma^0_{\rm VV}$ and low values of $\sigma^0_{\rm HV}$, and they decrease appreciably during crop growth. At a low incidence angle, the decreasing trend with plant height is due to the simultaneous increase of vegetation attenuation of the copolar scattering contribution from the soil and the increase of the cross-polarized volume scattering. Model simulations confirm that at low angles, crop growth produces a reduction of the $\sigma^0_{\rm VV}/\sigma^0_{\rm HV}$ ratio of about 7 dB, whereas soil-moisture variations from 0.1 to 0.4 produce effects on the order of 2 dB. It must be considered that single raining or drying events produce generally more limited variations of soil moisture.

Also note that the sensitivity of $\sigma^0_{\rm VV}/\sigma^0_{\rm HV}$ to height change is particularly large in the early part of the season, i.e., until the plants become 30 cm high. This is due to the effect of emerging leaves, although the total biomass is still very low. The decreasing trend, although with a lower slope, is maintained up to a maize height of about 2 m.

For the sake of comparison, we finally plotted the measured $\sigma^0_{\rm VV}/\sigma^0_{\rm HV}$ ratio versus the plant height of a wheat field in the Central Plain region. Fig. 13 shows that a decreasing trend, similar to the one of the maize, is also observed during the wheat growing period; however, a slight inversion of the trend

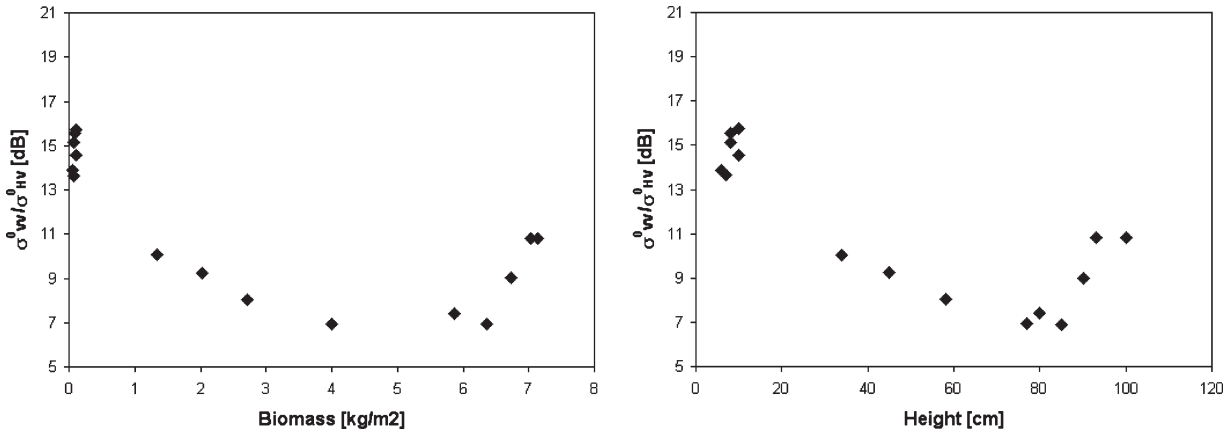

Fig. 13. Experimental trend of $\sigma^0_{\rm VV}/\sigma^0_{\rm HV}$ as a function of (left) biomass and (right) crop height for wheat at 2.5 GHz and 20° incidence angle.

of the polarization ratio, which is different from the maize case, is observed in the final stage. During the final earing stage (height values higher than about 80 cm), a slight further increase of height takes place simultaneously with drying, causing an increase of the polarization ratio.

V. Conclusion

This paper has shown the results of a systematic correlation study about the sensitivity of radar signatures to soil moisture and crop growth at several frequencies, angles, and combinations of polarizations. The analysis was carried out by means of backscattering data collected over a maize field, and it was supported by theoretical simulations performed with the Tor Vergata model.

The correlation analysis has shown that the highest sensitivities to SMC are reached by a vertical backscattering coefficient at low frequencies and low angles, whereas several configurations present large correlations with the maize biomass (or height), i.e., the co- and cross-polar ratios at intermediate frequencies and angles. On the other hand, experimental and modeling results indicate that a radar system operating at low frequency and low angles, at VV and HV polarizations, and with a sufficiently short revisit time has a good potential for both soil moisture and maize biomass monitoring, although vegetation scattering is more dominant at high angles. Indeed, the correlation study and the theoretical simulations showed that $\sigma^0_{\rm VV}$ is sensitive to soil moisture, whereas the cross-polarization ratio $\sigma^0_{\rm VV}/\sigma^0_{HV}$ presents a significant sensitivity to crop parameters and is moderately affected by soil-moisture variations.

References

[1] T. Le Toan, F. Ribbes, L.-F. Wang, N. Floury, K.-H. Ding, J. A. Kong, M. Fujita, and T. Kurosu, "Rice crop mapping and monitoring using ERS-1 data based on experiment and modeling results," *IEEE Trans. Geosci. Remote Sens.*, vol. 35, no. 1, pp. 41–56, Jan. 1997.

[2] F. Ribbes and T. Le Toan, "Rice field mapping and monitoring with RADARSAT data," *Int. J. Remote Sens.*, vol. 20, no. 4, pp. 745–765, 1999.

[3] A. Rosenqvist, "Temporal and spatial characteristics of irrigated rice in JERS-1 L-band SAR data," *Int. J. Remote Sens.*, vol. 20, no. 8, pp. 1567–1587, May 1999.

[4] P. Saich and M. Borgeaud, "Interpreting ERS SAR signatures of agricultural crops in Flevoland, 1993–1996," *IEEE Trans. Geosci. Remote Sens.*, vol. 38, no. 2, pp. 651–657, Mar. 2000.

[5] G. Cookmartin, P. Saich, S. Quegan, R. Cordey, P. Burgess-Allen, and A. Sowter, "Modeling microwave interactions with crops and comparison with ERS-2 SAR observations," *IEEE Trans. Geosci. Remote Sens.*, vol. 38, no. 2, pp. 658–670, Mar. 2000.

[6] A. Della Vecchia, P. Ferrazzoli, L. Guerriero, X. Blaes, P. Defourny, L. Dente, F. Mattia, G. Satalino, T. Strozzi, and U. Wegmüller, "Influence of geometrical factors on crop backscattering at C-band," *IEEE Trans. Geosci. Remote Sens.*, vol. 44, no. 4, pp. 778–790, Apr. 2006.

[7] K. A. Stankiewicz, "The efficiency of crop recognition on ENVISAT ASAR images in two growing seasons," *IEEE Trans. Geosci. Remote Sens.*, vol. 44, no. 4, pp. 806–814, Apr. 2006.

[8] G. Macelloni, S. Paloscia, P. Pampaloni, F. Marliani, and M. Gai, "The relationship between the backscattering coefficient and the biomass of narrow and broad leaf crops," *IEEE Trans. Geosci. Remote Sens.*, vol. 39, no. 4, pp. 873–884, Apr. 2001.

[9] F. Mattia, T. Le Toan, G. Picard, F. I. Posa, A. D'Alessio, C. Notarnicola, A. M. Gatti, M. Rinaldi, G. Satalino, and G. Pasquariello, "Multitemporal C-band radar measurements on wheat fields," *IEEE Trans. Geosci. Remote Sens.*, vol. 41, no. 7, pp. 1551–1560, Jul. 2003.

[10] [Online]. Available: http://www.congrex.nl/07c34/

[11] S. C. M. Brown, S. Quegan, K. Morrison, J. C. Bennett, and G. Cookmartin, "High-resolution measurements of scattering in wheat canopies—Implications for crop parameter retrieval," *IEEE Trans. Geosci. Remote Sens.*, vol. 41, no. 7, pp. 1602–1610, Jul. 2003.

[12] J. M. Lopez-Sanchez, J. D. Ballester-Berman, and J. Fortuny-Guasch, "Indoor wide-band polarimetric measurements on maize plants: A study of the differential extinction coefficient," *IEEE Trans. Geosci. Remote Sens.*, vol. 44, no. 4, pp. 758–767, Apr. 2006.

[13] J. L. Gomez-Dans, S. Quegan, and J. C. Bennett, "Indoor C-band polarimetric interferometry observations of a mature wheat canopy," *IEEE Trans. Geosci. Remote Sens.*, vol. 44, no. 4, pp. 768–777, Apr. 2006.

[14] J. M. Stiles and K. Sarabandi, "Electromagnetic scattering from grassland. I. A fully phase-coherent scattering model," *IEEE Trans. Geosci. Remote Sens.*, vol. 38, no. 1, pp. 339–348, Jan. 2000.

[15] A. Della Vecchia, P. Ferrazzoli, and L. Guerriero, "Modelling microwave scattering from long curved leaves," *Waves Random Media*, vol. 14, no. 2, pp. S333–S343, Apr. 2004.

[16] A. Della Vecchia, L. Guerriero, I. Bruni, and P. Ferrazzoli, "Hollow cylinder microwave model for stems," *J. Electromagn. Waves Appl.*, vol. 20, no. 3, pp. 301–318, 2006.

[17] X. Blaes, P. Defourny, U. Wegmüller, A. Della Vecchia, L. Guerriero, and P. Ferrazzoli, "C-band polarimetric indexes for maize monitoring based on a validated radiative transfer model," *IEEE Trans. Geosci. Remote Sens.*, vol. 44, no. 4, pp. 791–800, Apr. 2006.

[18] P. Ferrazzoli, "SAR for agriculture: Advances, problems and prospects (Keynote paper)," presented at the Proc. 3rd Int. Symp. on Retrieval of Bio- and Geophysical Parameters From SAR Data for Land Applications, pp. 47–56, Sheffield, U.K., 2002, Paper no. ESA SP 475.

[19] U. Wegmüller, "Remote sensing signature studies on agricultural fields with ground based radiometry and scatterometry," Ph.D. dissertation, Bern Univ., Berb, Switzerland, 1990.

[20] U. Wegmüller, "Signature research for crop classification by active and passive microwaves," *Int. J. Remote Sens.*, vol. 14, no. 5, pp. 871–883, Mar. 1993.
[21] M. Bracaglia, P. Ferrazzoli, and L. Guerriero, "A fully polarimetric multiple scattering model for crops," *Remote Sens. Environ.*, vol. 54, no. 3, pp. 170–179, Dec. 1995.
[22] F. T. Ulaby, R. K. Moore, and A. K. Fung, *Microwave Remote Sensing: Active and Passive*, vol. III. Norwood, MA: Artech House, 1986.
[23] H. J. Eom and A. K. Fung, "A scatter model for vegetation up to Ku-band," *Remote Sens. Environ.*, vol. 15, no. 3, pp. 185–200, Jun. 1984.
[24] D. M. Le Vine, R. Meneghini, R. H. Lang, and S. S. Seker, "Scattering from arbitrarily oriented dielectric disks in the physical optics regime," *J. Opt. Soc. Amer.*, vol. 73, no. 10, pp. 1255–1262, Oct. 1983.
[25] M. A. Karam and A. K. Fung, "Electromagnetic scattering from a layer of finite length, randomly oriented, dielectric, circular cylinders over a rough interface with application to vegetation," *Int. J. Remote Sens.*, vol. 9, no. 6, pp. 1109–1134, Jun. 1988.
[26] A. K. Fung, *Microwave Scattering and Emission Models and Their Applications*. Norwood, MA: Artech House, 1994.
[27] T.-D. Wu, K. S. Chen, J. Shi, and A. K. Fung, "A transition model for the reflection coefficient in surface scattering," *IEEE Trans. Geosci. Remote Sens.*, vol. 39, no. 9, pp. 2040–2050, Sep. 2001.
[28] Q. Li, J. Shi, and K. S. Chen, "A generalized power law spectrum and its applications to the backscattering of soil surfaces based on the integral equation model," *IEEE Trans. Geosci. Remote Sens.*, vol. 40, no. 2, pp. 271–280, Feb. 2002.
[29] A. K. Fung, Z. Li, and K. S. Chen, "Backscattering from a randomly rough dielectric surface," *IEEE Trans. Geosci. Remote Sens.*, vol. 30, no. 2, pp. 356–369, Mar. 1992.

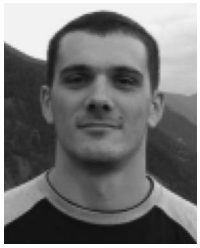

Andrea Della Vecchia received the B.S. (*cum laude*) and M.S. (*cum laude*) degrees in telecommunication engineering and the Ph.D. degree in geoinformation from Tor Vergata University, Rome, Italy, in 2001, 2002, and 2006, respectively.

His main research interest includes microwave remote sensing of vegetated terrains, with particular emphasis on electromagnetic modeling of backscattering and emissivity.

Paolo Ferrazzoli (M'94–SM'06) received the degree from the "La Sapienza" University of Rome, Rome, Italy, in 1972.

In 1974, he was with Telespazio S.p.A., where he was mainly active in the fields of antennas, slant-path propagation, and advanced satellite telecommunication systems. Since 1984, he has been with Tor Vergata University, Rome, where he is currently with the Department of Computer Science, Systems and Industrial Engineering, Faculty of Engineering, teaching microwaves and propagation. His research interest includes microwave remote sensing of vegetated terrains, with particular emphasis on electromagnetic modeling. He has been involved with international experimental remote-sensing campaigns such as AGRISAR, AGRISCATT, MAESTRO-1, MAC-Europe, and SIR-C/X-SAR. He has participated with the coordinating team of the European RAdar–Optical Research Assemblage Project, funded by the European Economic Community, establishing an assemblage among several European researchers working in radar applications.

Mr. Ferrazzoli is a member of the Science Advisory Group of the ESA SMOS Project.

Leila Guerriero received her "laurea" degree in physics from the "La Sapienza" University of Rome, Rome, Italy, in 1986 and the Ph.D. degree in electromagnetism from Tor Vergata University, Rome, Italy, in 1991.

In 1988, she was involved in a cooperation between the Jet Propulsion Laboratory and the Italian National Research Council for investigations on geophysical applications of Imaging Spectrometry in InfraRed and Visible Remote Sensing. In 1995, she participated in the ESA project concerning the radiometric polarimetry of the sea surface. In 1999–2001, she participated in the EEC concerted action European RAdar–Optical Research Assemblage, whose objective was to improve radar data analysis and utilization. More recently, she has been involved in the ESA project on the Use of Bistatic Microwave Measurements for Earth Observation. Since 1994, she has been a Permanent Researcher with Tor Vergata University, where she is now holding a course on satellite Earth monitoring. Her activities at Tor Vergata University are mainly concerned with modeling microwave backscattering and emissivity from agricultural and forested areas.

Luca Ninivaggi was born in Bari, Italy, in 1981. He received the B.S. and M.S. (graded with 110/110, *cum laude*) degrees in telecommunication engineering from Tor Vergata University, Rome, Italy, in 2004 and May 2006, respectively.

Since June 2006, he has been with Accenture, Rome, Italy, which is a telecommunication consulting company. He was with the Department of Computer Science, Systems and Industrial Engineering, Faculty of Engineering, Tor Vergata University.

Tazio Strozzi (M'98–SM'03) received the M.S. and Ph.D. degrees in physics from the University of Bern, Bern, Switzerland, in 1993 and 1996, respectively, for his experimental and theoretical studies on the backscattering characteristics of snow and vegetation.

From 1996 to 1998, he was a part-time Physics Teacher with a high school in Bellinzona, Switzerland. From 1999 to 2001, he was as part-time Visiting Scientist with the University of Wales, Swansea, U.K. He has been with GAMMA Remote Sensing AG, Muri, Switzerland, since 1996, where he is responsible for the development of radar remote-sensing applications and is the Manager of a number of research and commercial projects. His current activities include satellite SAR and SAR interferometry for land-use applications (including forest, urban areas, snow cover, and hazard mapping) and differential SAR interferometry from space and ground for glacier motion estimation, landslide surveying, and subsidence monitoring. He is a Principal Investigator for ENVISAT, ALOS PALSAR, and TerraSAR-X projects on subsidence and landslide monitoring.

Urs Wegmüller (M'94–SM'03) received the M.S. and Ph.D. degrees in physics from the University of Berne, Berne, Switzerland, in 1986 and 1990, respectively.

Between 1991 and 1992, he was with the Jet Propulsion Laboratory, Pasadena, CA, and between 1993 and 1995, with the University of Zürich, Zürich, Switzerland. Since 1995, he has been with GAMMA Remote Sensing AG (GAMMA), Gümligen, Switzerland, which is a Swiss company active in the development of signal-processing techniques and remote-sensing applications, where he was a Founding Member. Currently, as the Chief Executive Officer of GAMMA, he has overall responsibility for GAMMA's activities. At present, his main involvement is in the development of applications and the definition and implementation of related services in land-surface-deformation, hazard, land-use, and topographic mappings. He is/was the Principal Investigator for projects supported by ESA and the European Commission Framework programs.